

# Berry Phase Enforced Spinor Pairing Order

Yi Li and Grayson R. Frazier

Department of Physics and Astronomy, Johns Hopkins University, Baltimore, Maryland 21218, USA

(Dated: September 14, 2024)

We introduce a class of topological pairing orders characterized by a half-integer pair monopole charge, leading to Berry phase enforced half-integer partial wave symmetry. This exotic spinor pairing order can emerge from pairing between Fermi surfaces with Chern numbers differing by an odd integer. Using tight-binding models, we demonstrate spinor superconducting orders with monopole charges  $\pm 1/2$ , featuring a single gap node and nontrivial surface states. Additionally, the superfluid velocity follows a fractionalized Mermin-Ho relation in spatially inhomogeneous pairing orders. The concept extends to spinor density waves and excitons.

*Introduction.* – The discovery of a new pairing order is always accompanied by the establishment of a new paradigm to understand its physical properties and to probe the pairing symmetry. It has long been assumed that all pairing orders are completely classified by spherical harmonic symmetries and their lattice counterparts. Pioneering examples of unconventional superconductors and superfluids include  $p$ -wave superfluid  $^3\text{He}^{1-4}$ ,  $d$ -wave high- $T_c$  cuprates<sup>5-7</sup>, and  $s_{\pm}$ -wave iron pnictides<sup>8,9</sup>. Distinct symmetry of pairing gap functions gives rise to characteristic properties in different superconducting states. On the other hand, significant progress has been made in the discovery of topological quantum materials characterized by nontrivial geometric phases of single-particle electron bands<sup>10-14</sup> which lead to the discovery of, for example, quantum anomalous Hall insulators<sup>15-18</sup> and Weyl semimetals<sup>19-29</sup>.

Recently, monopole harmonic superconductivity<sup>30</sup> has been proposed based on generalization of the single-particle Berry phase to “pair Berry phase” – the two-particle Berry phase for Cooper pairs in superconductors<sup>31</sup>. This novel topological class of 3D superconductors can possibly exist in, for example, magnetic Weyl semimetals under the proximity effect with an ordinary  $s$ -wave superconductor. Generally, when pairing occurs between two Fermi surfaces of opposite Chern numbers, the inter-Fermi-surface Cooper pair can nontrivially inherit band topology and acquire a nontrivial “pair Berry phase” in the weak-coupling regime. The “pair Berry phase”, as a type of topological obstruction, prevents the gap function from being well defined over an entire Fermi surface. Hence, the corresponding gap function is no longer describable by spherical harmonic functions or their lattice counterparts. Instead, it is characterized by monopole harmonic functions, which are eigenfunctions of angular momentum in the presence of a magnetic monopole<sup>30,32-35</sup>. The “pair Berry phase” further enforces gap nodes and determines the total vorticity of gap nodes over a Fermi surface, independent of specific pairing mechanism. Therefore, monopole harmonic superconductivity fundamentally differs from previously known unconventional superconductivity. Furthermore, monopole harmonic superconductivity is only an example of topological many-particle order. In the particle-hole

channel, the monopole harmonic charge-density-wave (CDW) order<sup>36</sup> has been proposed in a model of Weyl semimetal consisting of nested Fermi surfaces that surround Weyl points of the same chirality. This novel topological class of CDW states is also characterized by monopole harmonic symmetry and can host emergent Weyl nodes in the gap functions.

In this article, we first explain the difference between the familiar examples of topological superfluid/superconductors<sup>2,4,37-44</sup> and the monopole harmonic superconductors. Then, we investigate the spinor pairing as an exotic example of monopole harmonic pairing states. When electrons pair between two topological Fermi surfaces carrying Chern numbers with different even- and oddness, the Cooper pair acquires a half-integer monopole charge. The gap function can exhibit an odd number of nodes over a single Fermi surface, leading to a nontrivial Bogoliubov excitation spectrum. We demonstrate the simplest example of an angular momentum  $j = 1/2$  spinor pairing order using tight-binding models in a cubic lattice, which exhibit a single Bogoliubov-de Gennes (BdG) gap node characterized by nontrivial chirality, providing a nontrivial example of a general result that the Nielsen-Ninomiya theorem<sup>45,46</sup> does not hold in lattice systems when U(1) symmetry is broken. Furthermore, we show zero energy Majorana surface states arising from momentum space phase winding of the low-energy spinor pairing order in the bulk. Lastly, we show that the superfluid velocity obeys a fractional generalization of the Mermin-Ho relation<sup>47</sup> in the presence of spatial inhomogeneity of order parameters.

*Monopole harmonic pairing and complex  $d$ -vectors.* – We begin with examples of topological superconductivity where the Fermi surface is topologically trivial, but the superconducting gap function exhibits nontrivial topology. For example, the spin-polarized  $p_x + ip_y$  pairing is fully gapped in 2D. It belongs to class  $D$ , which breaks both spin-rotation and time-reversal symmetry. The gap function  $\Delta(\mathbf{k})$  is a complex function exhibiting a phase winding number  $\nu = \frac{1}{2\pi} \oint d\mathbf{k} \partial_{\mathbf{k}} \theta(\mathbf{k})$  around the 1D Fermi circle, where  $\theta(\mathbf{k})$  is the U(1) phase of the gap function. The 3D time-reversal invariant pairing of the  $^3\text{He-B}$  type belongs to class DIII, and the single-particle band structure exhibits two-fold spin degeneracy. The

corresponding gap function is no longer a scalar but is represented by a pairing matrix. It is proportional to a  $2 \times 2$  unitary matrix, say,  $\Delta(\mathbf{k}) = i\sigma_y \hat{\mathbf{d}}(\mathbf{k}) \cdot \boldsymbol{\sigma}$ , where the real  $d$ -vector exhibits a nontrivial texture over the Fermi surface characterized by a nontrivial Pontryagin index,

$$\nu = \frac{1}{8\pi} \oint_{\text{FS}} d^2k \epsilon_{\mu\nu} \hat{\mathbf{d}}(\mathbf{k}) \cdot \partial_{k_\mu} \hat{\mathbf{d}}(\mathbf{k}) \times \partial_{k_\nu} \hat{\mathbf{d}}(\mathbf{k}). \quad (1)$$

Under an open boundary condition, 2D C-class topological superconductors exhibit 1D chiral Majorana modes on the edge, while 3D DIII-class time-reversal invariant topological superconductors exhibit helical 2D Majorana surface modes.

Recently, monopole superconductivity<sup>30</sup> has been proposed as a novel topological class of superconducting pairing order. The central idea is that when Cooper pairing occurs between two Fermi surfaces of different Chern numbers, the resulting Cooper pairs acquire a nontrivial two-particle pair Berry phase, which introduces topological obstruction in the U(1) phase of the pairing order. For example, consider the simplest model of a Weyl semimetal state with a pair of Weyl points located at  $\pm \mathbf{K}_0$ . Upon doping, the Weyl points are enclosed by two separated Fermi surfaces, denoted  $\text{FS}_{c,\pm}$ . Near these Fermi surfaces, the low-energy Hamiltonians take the form  $H_{\pm}(\mathbf{k} \mp \mathbf{K}_0) = \pm v_F \mathbf{k} \cdot \boldsymbol{\sigma} - \mu$ . The Fermi surfaces  $\text{FS}_{c,\pm}$  exhibit nontrivial single-particle Berry phases, with single-particle monopole charges being  $\pm q = \mp 1/2$ . Alternatively, the corresponding Chern numbers are  $\pm C$  with  $C = 2q$ . For the pairing between  $\text{FS}_{c,+}$  and  $\text{FS}_{c,-}$ , the gap function can be represented by a  $2 \times 2$  pairing matrix in the spin- $\uparrow, \downarrow$  basis. Monopole pairing is an example of *nonunitary* pairing, characterized by complex  $\mathbf{d}$ -vectors  $(-d_x + id_y)/\sqrt{2} = u_k^2$ ,  $(d_x + id_y)/\sqrt{2} = v_k^2$ ,  $d_z = \sqrt{2}u_k v_k$ , where  $u_k = \cos \frac{\theta_k}{2}$  and  $v_k = \sin \frac{\theta_k}{2} e^{i\phi_k}$ . The pair Berry connection can be defined in terms of complex  $\mathbf{d}$ -vectors as

$$\mathbf{A}_{pair}(\mathbf{k}) = \hat{\mathbf{d}}^* i \nabla_{\mathbf{k}} \hat{\mathbf{d}} = 2q_{pair} \tan \frac{\theta_{\mathbf{k}}}{2} \hat{e}_{\phi_{\mathbf{k}}}. \quad (2)$$

Correspondingly, the Berry curvature can be expressed as  $\Omega_i(\mathbf{k}) = \epsilon_{ijl} \partial_j A_{pair,l} = i \epsilon_{ijl} \partial_j \hat{\mathbf{d}}^* \cdot \partial_l \hat{\mathbf{d}}$ . The total pair Berry flux through  $\text{FS}_{c,+}$  is

$$\oint_{S_+} d\mathbf{k} \cdot \nabla_{\mathbf{k}} \times \mathbf{A}_p(\mathbf{k}) = \oint_{S_+} d\mathbf{k} \cdot i \partial_j \hat{\mathbf{d}}^* \times \partial_k \hat{\mathbf{d}} = 4\pi q_{pair}. \quad (3)$$

where the pair monopole charges  $q_{pair} = 2q$ . Hence, the inter-Fermi-surface pairing inherits the Berry phases of electrons residing on different topological Fermi surfaces in a nontrivial way.

As a result, the topological obstruction in the wavefunction of Cooper pairs prevents its phase from being well defined over an entire Fermi surface, leading to generic nodal structures in the pairing gap functions. The gap function  $\Delta(\mathbf{k})$ , when projected onto  $\text{FS}_{c,\pm}$ ,

exhibits a nodal structure with total vorticity  $2q_{pair}$  in momentum space, which is independent of specific pairing mechanisms<sup>30</sup>. When  $q_{pair} \neq 0$ ,  $\Delta(\mathbf{k})$  cannot be a regular function throughout the  $\text{FS}_{c,+}$ . This nodal structure is fundamentally different from that of familiar pairing symmetries based on spherical harmonics  $Y_{lm}(\hat{\mathbf{k}})$ , which are well defined on the entire Fermi surface and correspond to  $q_{pair} = 0$  with zero total vorticity. For example, in the <sup>3</sup>He-A type  $p_x + ip_y$  pairing in 3D, the gap nodes appear at the north and south poles of the Fermi surface as a pair of momentum space vortex and antivortex, respectively.

Away from the Fermi surface, the nodes of  $\Delta(\mathbf{k})$  extend into vortex lines in momentum space. The Weyl points of opposite chiralities are sources and drains for the fundamental vortex lines that intersect the Fermi surface, forming vortices and antivortices in momentum space with a total vorticity of  $\pm 2q_{pair}$ . Vortex lines that do not connect to Weyl points form closed loops and are nonfundamental - their intersections with the Fermi surfaces create pairs of vortices and antivortices which are not enforced by topology but enrich the symmetry of the pairing order. A remarkable feature of this system is that even though these band Weyl points are at high energy near the cutoff scale, far away from the Fermi energy after doping, the non-perturbative nature of topological properties governs the low-energy nodal excitations of  $\Delta(\mathbf{k})$  which inherit band topology in a nontrivial way.

*Spinor pairing from half-integer pair monopole charges.* - So far, we have only discussed monopole pairing with integer-valued monopole charges  $q_{pair}$ , where the pairing symmetry remains within integer partial-wave channels. However, when pairing occurs between two Fermi surfaces with Chern numbers differing by an odd integer, the resulting pair monopole charge  $q_{pair} = |C_1 - C_2|/2$  becomes a half-integer. A notable feature of this pairing is that the order parameter, typically assumed to be bosonic, actually forms a spinor representation of rotation symmetry.

Consider a system consisting of two different types of fermions. The first type is a spin-1/2 fermion, with annihilation operators denoted by  $c_{\alpha}$ ,  $\alpha = \uparrow, \downarrow$  and mass  $m$ . This fermion has a 3D Weyl-type spin-orbit coupling as described by  $H_c^0$ . The second type of fermion, described by  $H_d^0$ , is a single-component fermion with annihilation operators denoted by  $d$  and mass  $M$ . It exhibits a simple parabolic dispersion.

$$\begin{aligned} H_c^0 &= \sum_{\mathbf{k}} \sum_{\alpha, \beta = \uparrow, \downarrow} c_{\alpha}^{\dagger}(\mathbf{k}) \left( \frac{\hbar^2 k^2}{2m} - \lambda \mathbf{k} \cdot \boldsymbol{\sigma}_{\alpha\beta} - \mu_c \right) c_{\beta}(\mathbf{k}), \\ H_d^0 &= \sum_{\mathbf{k}} d^{\dagger}(\mathbf{k}) \left( \frac{\hbar^2 k^2}{2M} - \mu_d \right) d(\mathbf{k}). \end{aligned} \quad (4)$$

The synthetic spin-orbit coupling of  $c$  fermion has been proposed for realization in ultracold atom systems via light-atom interactions<sup>48,49</sup>. This system breaks inversion symmetry, resulting in split Fermi surfaces,

labeled as  $\text{FS}_{c,\pm}$ , which possess opposite monopole charges,  $q_c = \pm 1/2$ . The Fermi wavevectors,  $k_{F;c,\pm}$  and  $k_{F;d}$ , corresponding to the three Fermi surfaces, satisfy  $k_{F;c,\pm}^2/2m \pm \lambda k_{F;c,\pm} = \mu_c$  and  $k_{F;d}^2/2M = \mu_d$ .

To facilitate pairing between the  $c$  and  $d$  Fermi surfaces, consider the simplest scenario where the Fermi surface of  $d$  fermion,  $\text{FS}_d$ , matches with one of the helical Fermi surfaces of  $c$  fermion, say  $\text{FS}_{c,+}$ . This can be achieved by tuning the chemical potential  $\mu_d$  of  $d$  fermions such that  $k_{F;d} = k_{F;c,+}$ . In this case, Cooper pairing can occur between  $\text{FS}_{c,+}$  and  $\text{FS}_d$ , which possess Chern numbers of  $-1$  and  $0$ , respectively. The mean-field inter-Fermi-surface pairing Hamiltonian takes the form

$$H_\Delta = \sum_{\mathbf{k}; \alpha=\uparrow, \downarrow} \Delta_\alpha(\mathbf{k}) c_\alpha^\dagger(\mathbf{k}) d^\dagger(-\mathbf{k}) + \Delta_\alpha^*(\mathbf{k}) d(-\mathbf{k}) c_\alpha(\mathbf{k}). \quad (5)$$

Here, the gap function takes a two-component form  $\mathbf{\Delta}(\mathbf{k}) = (\Delta_\uparrow(\mathbf{k}), \Delta_\downarrow(\mathbf{k}))^T$ . Since the kinetic Hamiltonian preserves spin orbit coupled rotational symmetry, the pairing gap function can be expanded in terms of partial wave channels of half-integer angular momentum quantum numbers  $j$  and  $j_z$  as  $\mathbf{\Delta}(\mathbf{k}) = \sum_{j, j_z} \mathbf{\Delta}_{j, j_z}(\mathbf{k})$ . Due to broken inversion symmetry, each partial wave pairing channel with angular momentum  $j$  and  $j_z$  is generally a superposition of two orbital angular momentum channels of opposite parity,  $l = j - 1/2$  and  $l + 1 = j + 1/2$ :  $\Delta_{jj_z; \alpha}(\mathbf{k}) = \Delta_{jj_z; l, \alpha}(\mathbf{k}) + \Delta_{jj_z; l+1, \alpha}(\mathbf{k})$  with  $\Delta_{jj_z; l, \alpha}(\mathbf{k}) = \Delta_{jj_z; l}(k) \phi_{jj_z; l, \alpha}(\hat{\mathbf{k}})$ . Here,  $\Delta_{jj_z; l}(k)$  is the pairing amplitude and  $\phi_{jj_z; l, \alpha}(\hat{\mathbf{k}}) = \langle jj_z | l, m; \frac{1}{2}, \alpha \rangle Y_{lm}(\hat{\mathbf{k}}) \otimes |\alpha\rangle$  is the  $\alpha = \uparrow, \downarrow$  component of spin spherical harmonic function<sup>50</sup>.

To understand the pairing at low energy near Fermi surfaces, we note that states at  $\text{FS}_{c,\pm}$  are respectively described by the helical band eigenstates  $|\lambda_\pm(\mathbf{k})\rangle$  for  $c$  fermions. They satisfy  $\boldsymbol{\sigma} \cdot \hat{\mathbf{k}} |\lambda_\pm(\mathbf{k})\rangle = \pm |\lambda_\pm(\mathbf{k})\rangle$ . When  $\text{FS}_d$  matches with  $\text{FS}_{c,+}$ , at low energy, the spin spherical harmonics in the pairing order are projected to monopole harmonics as  $P^{(+)}\phi_{jj_z; l, \alpha}(\hat{\mathbf{k}}) = -P^{(+)}\phi_{jj_z; l+1, \alpha}(\hat{\mathbf{k}}) = \frac{1}{\sqrt{2}} Y_{q_{pair}; j, j_z}(\hat{\mathbf{k}})$ , where  $q_{pair} = -1/2$ ,  $j = l + 1/2$ , and  $Y_{q_{pair}; j, j_z}(\hat{\mathbf{k}})$  is the monopole harmonic function. It satisfies  $J^2 Y_{q_{pair}; j, j_z} = j(j+1) Y_{q_{pair}; j, j_z}$  and  $J_z Y_{q_{pair}; j, j_z} = j_z Y_{q_{pair}; j, j_z}$  with  $j = |q_{pair}|, |q_{pair}| + 1, \dots$  and  $|j_z| \leq j$  (see Supplemental Material (S.M.) S1 for details). Consequently, the gap function  $\mathbf{\Delta}(\mathbf{k})$  becomes a function of half charge monopole harmonics,  $\Delta^{(+)}(\mathbf{k}) = \sum_{j, j_z} \Delta_{jj_z} Y_{q_{pair}=-1/2; j, j_z}(\hat{\mathbf{k}})$  where  $\Delta_{jj_z} = (\Delta_{jj_z; l=j-1/2}(k) - \Delta_{jj_z; l=j+1/2}(k))/\sqrt{2}$ . The projected pairing Hamiltonian then takes the form

$$H_\Delta^{(+)}(\mathbf{k}) = \sum_{j, j_z} \Delta_{jj_z} Y_{q_{pair}=-1/2; j, j_z}(\hat{\mathbf{k}}) \chi_+^\dagger(\mathbf{k}) d^\dagger(-\mathbf{k}) + \text{h.c.}, \quad (6)$$

where,  $\chi_+^\dagger(\mathbf{k}) = \sum_{\alpha=\uparrow, \downarrow} \lambda_{+, \alpha}(\mathbf{k}) c_\alpha^\dagger(\mathbf{k})$  is the creation operator of a single band eigenstate at  $\mathbf{k}$  on  $\text{FS}_{c,+}$ .

We emphasize that, regardless of specific interactions in the pairing mechanism, the pairing order always

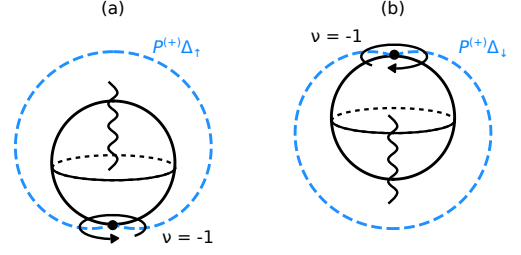


FIG. 1. (Color online) Spinor pairing gap functions (a)  $P^{(+)}\Delta_\uparrow \propto Y_{-\frac{1}{2}; \frac{1}{2}, \frac{1}{2}}(\hat{\mathbf{k}})$  and (b)  $P^{(+)}\Delta_\downarrow \propto Y_{-\frac{1}{2}; \frac{1}{2}, -\frac{1}{2}}(\hat{\mathbf{k}})$  (blue, dashed) overlaid onto Fermi surface  $\text{FS}_{c,+}$  (black, solid). They exhibit local chiral  $p$ -wave symmetry near the gap node under the choice of gauge with Dirac string (wavy line) going through the antipodal point in  $\text{FS}_{c,+}$ .

exhibits half-integer charged monopole pairing, following singular spinor representations. For instance, consider the simplest case of an attractive contact interaction between these two types of fermions,

$$H_{int} = -g \int d\mathbf{r} c_\alpha^\dagger(\mathbf{r}) d^\dagger(\mathbf{r}) d(\mathbf{r}) c_\alpha(\mathbf{r}), \quad (7)$$

which would only give rise to conventional  $s$ -wave pairing when Fermi surfaces are topologically trivial. In this case, before projection,  $\Delta_{\alpha=\uparrow, \downarrow} = -\frac{g}{V} \int d\mathbf{r} \langle G | d(\mathbf{r}) c_\alpha(\mathbf{r}) | G \rangle$  is a constant independent of  $\hat{\mathbf{k}}$ . Nevertheless, after the projection, the gap functions  $\Delta_{\alpha=\uparrow, \downarrow}$  become

$$P^{(+)}\Delta_\uparrow = \sqrt{2\pi} \Delta Y_{-\frac{1}{2}; \frac{1}{2}, \frac{1}{2}}(\hat{\mathbf{k}}) = \Delta \cos \frac{\theta_{\mathbf{k}}}{2} e^{i\phi_{\mathbf{k}}},$$

$$P^{(+)}\Delta_\downarrow = \sqrt{2\pi} \Delta Y_{-\frac{1}{2}; \frac{1}{2}, -\frac{1}{2}}(\hat{\mathbf{k}}) = \Delta \sin \frac{\theta_{\mathbf{k}}}{2} e^{-i\phi_{\mathbf{k}}}, \quad (8)$$

which are time reversal partners with each other. As shown in Fig. 1 (a-b), the projected gap function  $P^{(+)}\Delta_\uparrow$  ( $P^{(+)}\Delta_\downarrow$ ) exhibits a single point node at the south (north) pole on  $\text{FS}_{c,+}$ . Locally, we describe the monopole spinor pairing order as familiar chiral  $p$ -wave by choosing a gauge in which the pairing order is well-defined at the respective nodal point. The corresponding single gap node contributes to nonvanishing total vorticity in momentum space,  $\nu = \frac{1}{2\pi} \oint_C d\mathbf{k} \cdot \mathbf{v} = 2q_{pair} = -1$ . Here,  $\mathbf{v}(\mathbf{k}) = \nabla_{\mathbf{k}} \phi(\mathbf{k}) - \mathbf{A}_p(\mathbf{k})$  is the gauge-invariant “velocity” in momentum space.

Analogous to the concept of composite fermions<sup>51</sup>, this monopole spinor pairing order can be described as a composite order characterized by a local chiral  $p$ -wave order under a specific gauge choice combined with a nonlocal Dirac string. The Dirac string introduces a Berry flux which shifts the angular momentum of the composite pairing order, leading to a spinor representation with gauge invariant half-integer pairing angular momentum. Moreover, this monopole spinor pairing order can be extended to describe spinor density waves and spinor excitons in the particle-hole channel.

Next, we study the Bogoliubov quasiparticle excitations. As an example, we consider the case of  $q_{pair} =$

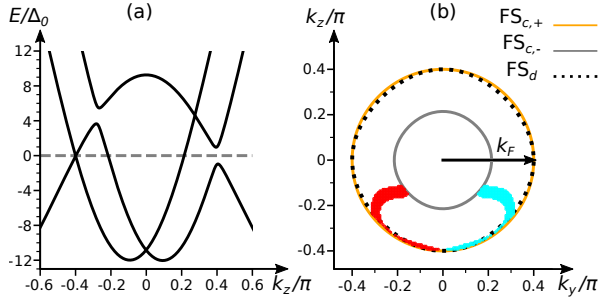


FIG. 2. (Color online) (a) Bulk BdG spectrum of the three-band tight-binding model of spinor superconductor in Eq. (10) along the  $k_z$  axis. It exhibits a single BdG Weyl node at  $k_z = -0.4\pi$ . (b) zero energy surface arcs (colored) within 2D surface Brillouin zone. States localized at  $x = 0$  ( $x = L_x$ ) are shown in red (cyan). Overlaid are the  $k_x = 0$  cross sections of bulk Fermi surfaces,  $FS_d$  (dashed black line),  $FS_{c,+}$  (solid orange line), and  $FS_{c,-}$  (solid gray line). Parameters are  $t = -1$ ,  $t_d/t = 1$ ,  $t_c/t = 2$ ,  $\mu_d/t = 4.62$ ,  $\mu_c/t = 10.38$ ,  $\lambda/|t| = 1.20$ ,  $k_F = 0.4\pi$ , and  $L_x = 300$ . The pairing is given by  $\Delta = (\Delta_0, 0)^T$ , with  $\Delta_0/|t| = 0.15$ .

$-1/2$ ,  $j = j_z = 1/2$ , which occurs when inter-Fermi surface pairing between  $FS_{c,+}$  and  $FS_d$  takes the form  $\Delta = (\Delta_0, 0)^T$ , with  $\Delta_0$  being the pairing amplitude. In the Nambu basis  $\psi(\mathbf{k}) = (\chi_+(\mathbf{k}), d^\dagger(-\mathbf{k}))^T$ , we have

$$\mathcal{H}(\mathbf{k}) = \epsilon_{0,k}\tau_0 + \epsilon_k\tau_3 + \Delta_0\sqrt{2\pi}Y_{-\frac{1}{2};\frac{1}{2};\frac{1}{2}}(\hat{\mathbf{k}})\tau_+ + \Delta_0\sqrt{2\pi}Y_{-\frac{1}{2};\frac{1}{2};\frac{1}{2}}^*(\hat{\mathbf{k}})\tau_-, \quad (9)$$

where  $\tau_\pm = (\tau_x \pm i\tau_y)/2$ . Here,  $\epsilon_{0,k} = (\epsilon_{k;c,+} - \epsilon_{k;d})/2$  and  $\epsilon_k = (\epsilon_{k;c,+} + \epsilon_{k;d})/2$ , with  $\epsilon_{k;c,+} = \hbar^2 k^2/(2m) - \lambda k - \mu_c$  and  $\epsilon_{k;d} = \hbar^2 k^2/(2M) - \mu_d$  being the dispersions of the band eigenstates at the Fermi level. The Bogoliubov quasiparticle excitations are  $\gamma_1^\dagger(\mathbf{k}) = \cos \frac{\beta_k}{2} \chi^\dagger(\mathbf{k}) + \sin \frac{\beta_k}{2} d(-\mathbf{k})$ ,  $\gamma_2^\dagger(\mathbf{k}) = \sin \frac{\beta_k}{2} d(\mathbf{k}) - \cos \frac{\beta_k}{2} \chi^\dagger(-\mathbf{k})$ , where  $\tan \beta_k = \sqrt{2\pi}\Delta_0 Y_{-\frac{1}{2};\frac{1}{2};\frac{1}{2}}(\hat{\mathbf{k}})/\epsilon_k$ . The corresponding excitation spectrum is  $E(\mathbf{k}) = \epsilon_{0,k} \pm \sqrt{\epsilon_k^2 + \Delta_0^2 \cos^2(\theta_{\mathbf{k}}/2)}$ . When pairing is instead  $\Delta = (0, \Delta_0)$ , corresponding to  $j_z = -1/2$  channel, we have  $E(\mathbf{k}) = \epsilon_{0,k} \pm \sqrt{\epsilon_k^2 + \Delta_0^2 \sin^2(\theta_{\mathbf{k}}/2)}$ . The two pairings exhibit a single BdG node at the south or north pole, respectively.

*Tight-binding models.* – To further demonstrate the exotic spinor pairing and its surface states, we consider a tight-binding Hamiltonian with the kinetic part  $\mathcal{H}_{c;t.b.}^0(\mathbf{k}) = \sum_i (2t_c \cos k_i \mathbb{1} - \lambda \sin k_i \sigma_i) - \mu_c \mathbb{1}$  and  $\mathcal{H}_{d;t.b.}^0(\mathbf{k}) = \sum_i 2t_d \cos k_i - \mu_d$ , and on-site pairing between  $c$  and  $d$  fermions. It takes the following form,

$$H_{t.b.} = \sum_{\mathbf{n}, \mathbf{n}'} \Psi_{\mathbf{n}}^\dagger \left( \begin{array}{c|c} [\mathcal{H}_c^0]_{\mathbf{n}, \mathbf{n}'} & \Delta_\uparrow \delta_{\mathbf{n}, \mathbf{n}'} \\ \Delta_\downarrow \delta_{\mathbf{n}, \mathbf{n}'} & -[\mathcal{H}_d^0]_{\mathbf{n}, \mathbf{n}'} \end{array} \right) \Psi_{\mathbf{n}'}. \quad (10)$$

Here,  $\Psi_{\mathbf{n}} = (c_{\mathbf{n},\uparrow}, c_{\mathbf{n},\downarrow}, d_{\mathbf{n}}^\dagger)^T$ , with  $c_{\mathbf{n},\sigma}$  ( $d_{\mathbf{n}}$ ) being the

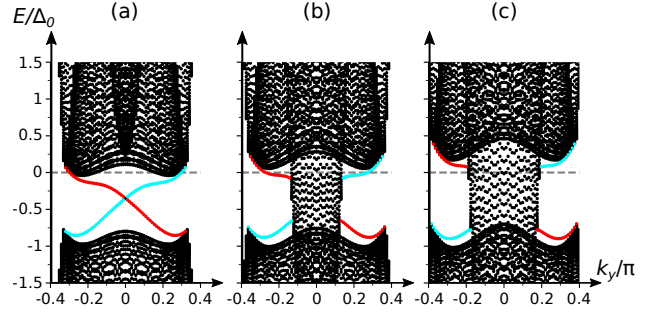


FIG. 3. (Color online) Energy dispersion of surface modes in Fig. 2 (b) at (a)  $k_z = -0.22\pi$ , (b)  $k_z = -0.16\pi$  where surface modes merge into bulk spectrum (black) for  $|k_y| < k_{F;c,-}$ , and (c)  $k_z = -0.10\pi$  where only bulk states of unpaired  $FS_{c,-}$  reside at zero energy. The color scheme for surface states and parameters are the same as those in Fig. 2 (b).

annihilation operator of  $c$  fermion with spin  $\sigma$  (spinless  $d$  fermion) at site  $\mathbf{n}$  in a cubic lattice. Nonzero matrix elements of  $\mathcal{H}_c^0$  and  $\mathcal{H}_d^0$  are  $[\mathcal{H}_c^0]_{\mathbf{n}, \mathbf{n}} = -\mu_c \mathbb{1}_{2 \times 2}$ ,  $[\mathcal{H}_c^0]_{\mathbf{n}, \mathbf{n} + \delta_i} = t_c \mathbb{1}_{2 \times 2} - \frac{i}{2} \lambda [\sigma_i]_{2 \times 2}$ ,  $[\mathcal{H}_d^0]_{\mathbf{n}, \mathbf{n}} = -\mu_d$ , and  $[\mathcal{H}_d^0]_{\mathbf{n}, \mathbf{n} + \delta_i} = t_d$ . Here,  $\delta_i$  denotes the direct lattice vector of unit length between nearest neighboring sites along  $i = x, y, z$ .  $t_c$  and  $t_d$  are spin-independent hopping amplitudes for  $c$  and  $d$  fermions, respectively, and  $\lambda$  is the spin-orbit coupling strength. For  $\mathcal{H}_c^0$ , we take a convention in the tensor product representation that the two-dimensional spin- $\uparrow, \downarrow$  basis is nested under lattice site basis. To satisfy the Fermi surface matching condition to pair  $FS_{c,+}$  with  $FS_d$ , we take  $\mu_d = 2t_d(\cos k_F + 2)$  and  $\mu_c = 2t_c(\cos k_F + 2) + \lambda |\sin k_F|$ , with  $k_F = k_{F;c,+} = k_{F;d}$  being the Fermi wavevector at the overlap of  $FS_{c,+}$  and  $FS_d$ , as shown in Fig. 2 (b).

To demonstrate spinor pairing at  $j_z = 1/2$  channel, we take  $\Delta_\uparrow = \Delta_0$  and  $\Delta_\downarrow = 0$ . The bulk BdG spectrum of the system is shown in Fig. 2 (a), which exhibits a single point node at the south pole of the overlapped Fermi surfaces  $FS_{c,+}$  and  $FS_d$ . Near the south pole  $(0, 0, -k_F)$ , the low-energy BdG Hamiltonian in the  $(\chi_+(\mathbf{k}), d^\dagger(-\mathbf{k}))^T$  Nambu basis takes the form  $\mathcal{H}(\mathbf{k}) \equiv \mathcal{H}(\tilde{\mathbf{k}} - k_F \hat{z}) \approx \begin{pmatrix} -v_1 \tilde{k}_z & v_\parallel (\tilde{k}_x + i\tilde{k}_y) \\ v_\parallel (\tilde{k}_x - i\tilde{k}_y) & v_2 \tilde{k}_z \end{pmatrix}$  with  $v_\parallel = \Delta_0/(2|\sin k_F|)$ ,  $v_1 = -2t_c \sin k_F + \lambda \cos k_F > 0$ , and  $v_2 = -2t_d \sin k_F > 0$ . It exhibits an emergent BdG Weyl node with chirality  $-1$ . This is a nontrivial example of a general statement that the Nielsen-Ninomiya theorem does not hold in lattice systems when  $U(1)$  symmetry is broken<sup>46</sup>.

Furthermore, the nontrivial phase winding near the gap node gives rise to zero energy surface modes localized at opposite sides of the system, as shown in Fig. 2 (b). These nontrivial surface states originate from the location of the pairing gap node and merge into the zero energy bulk states of the unpaired  $FS_{c,-}$  as shown in Fig. 3 (a-c). In contrast to, for example,



a three-dimensional  $p_x + ip_y$  superconductor, where the zero energy surface mode arc resides between the vortex and antivortex at the two poles of the Fermi surface, the surface mode in this spinor superconductor is only connected to the single gap node and merges into the unpaired Fermi surface. When pairing occurs between  $\text{FS}_{c,-}$  and  $\text{FS}_d$ , we have similar results for the spinor pairing with opposite pair monopole charge, as shown in Sec. S2 of S.M.

*Fractional Mermin-Ho relation.* – Lastly, we explore the situation of inhomogeneous spatial distribution of the spinor pairing order. Consider the simplest case where, before projection, the pairing gap function  $\Delta(\mathbf{r}) = |\Delta(\mathbf{r})|e^{i\phi(\mathbf{r})}\eta(\mathbf{r})$ , where  $\eta(\mathbf{r})$  is a fundamental spin-1/2 spinor. In momentum space,  $\eta$  is projected to the monopole harmonic function  $P_+\eta = \eta_\alpha Y_{-\frac{1}{2};\frac{1}{2},\alpha}(\hat{\mathbf{k}})$ . Through Hopf map, the spinor gap function is mapped to a unit 3-vector as  $\hat{\mathbf{n}}(\mathbf{r}) = \eta^\dagger \boldsymbol{\sigma} \eta$ . In  $^3\text{He}$ - $A$   $p$ -wave superfluid, the direction of Cooper pairing orbital angular momentum is denoted by the  $\mathbf{l}$ -vector, and the curl of the superfluid velocity is determined by the spatial variation of  $\mathbf{l}$ -vector via  $(\nabla \times \nabla \phi(\mathbf{r}))_i = \epsilon_{ijk} \hat{\mathbf{l}} \cdot \partial_j \hat{\mathbf{l}} \times \partial_k \hat{\mathbf{l}}$ , which is the celebrated Mermin-Ho relation<sup>47</sup>. Here, for the spinor pairing order, the corresponding Mermin-Ho relation is fractionalized. The spatial variation of  $\hat{\mathbf{n}}$  leads to the following nontrivial circulation of the superfluid velocity

$$(\nabla \times \nabla \phi(\mathbf{r}))_i = \frac{1}{2} \epsilon_{ijk} \hat{\mathbf{n}} \cdot \partial_j \hat{\mathbf{n}} \times \partial_k \hat{\mathbf{n}}. \quad (11)$$

In a spherical harmonic trap, there will appear a single vortex on the boundary induced by geometric curvature.

In summary, we have studied a class of topological nodal superconducting states characterized by a nontrivial two-particle pairing Berry phase. The low-energy gap function is described by monopole harmonic functions, not only in the integer monopole charge channels but also in more exotic half-integer monopole charge channels. The half-integer monopole pairing order follows spinor representation, even though it arises from Cooper pairs which are bosonic. The Berry phase enforced spinor pairing order can exist in, for example, ultra-cold atom systems with synthetic spin-orbit coupling, when Cooper pairing occurs between two Fermi surfaces with Chern numbers differing by an odd integer. Furthermore, we have demonstrated the 1/2 monopole charge spinor superconducting order in a lattice. The system exhibits single BdG Weyl node in the bulk spectrum and exotic surface states arising from nontrivial phase winding of spinor pairing order about the gap node. Lastly, when the spinor pairing order parameter has a spatial gradient, the superfluid velocity ceases to be irrotational, and a fractional version of the Mermin-Ho relation has been derived.

*Acknowledgments* – Y.L. acknowledges the support by the U.S. Department of Energy, Office of Basic Energy Sciences, Division of Materials Sciences and Engineering, Grant No. DE-SC0019331 and the support of the Alfred P. Sloan Research Fellowships, under which the concept of spinor pairing was developed. Y.L. and G.R.F. acknowledge the support by the NSF CAREER Grant No. DMR-1848349 for developing the tight-binding model and studying the surface states of the spinor monopole pairing order.

- 
- <sup>1</sup> P.W. Anderson and P. Morel, “Generalized bardeen-cooper-schrieffer states and the proposed low-temperature phase of liquid  $\text{He}^3$ ,” *Phys. Rev.* **123**, 1911 (1961).
- <sup>2</sup> R. Balian and N.R. Werthamer, “Superconductivity with pairs in a relative  $p$  wave,” *Phys. Rev.* **131**, 1553 (1963).
- <sup>3</sup> Anthony J. Leggett, “A theoretical description of the new phases of liquid  $^3\text{He}$ ,” *Rev. Mod. Phys.* **47**, 331–414 (1975).
- <sup>4</sup> Grigory E. Volovik, *The universe in a helium droplet*, Vol. 117 (Oxford University Press, 2003).
- <sup>5</sup> C. C. Tsuei, J. R. Kirtley, C. C. Chi, Lock See Yu-Jahnes, A. Gupta, T. Shaw, J. Z. Sun, and M. B. Ketchen, “Pairing symmetry and flux quantization in a tricrystal superconducting ring of  $\text{YBa}_2\text{Cu}_3\text{O}_7$ ,” *Phys. Rev. Lett.* **73**, 593–596 (1994).
- <sup>6</sup> D. J. Van Harlingen, “Phase-sensitive tests of the symmetry of the pairing state in the high-temperature superconductors—evidence for  $d_{x^2-y^2}$  symmetry,” *Rev. Mod. Phys.* **67**, 515–535 (1995).
- <sup>7</sup> C. C. Tsuei and J. R. Kirtley, “Pairing symmetry in cuprate superconductors,” *Rev. Mod. Phys.* **72**, 969–1016 (2000).
- <sup>8</sup> G. R. Stewart, “Superconductivity in iron compounds,” *Rev. Mod. Phys.* **83**, 1589–1652 (2011).
- <sup>9</sup> Pengcheng Dai, “Antiferromagnetic order and spin dynamics in iron-based superconductors,” *Rev. Mod. Phys.* **87**, 855–896 (2015).
- <sup>10</sup> F. D. M. Haldane, “Model for a quantum hall effect without landau levels: Condensed-matter realization of the “parity anomaly”,” *Phys. Rev. Lett.* **61**, 2015–2018 (1988).
- <sup>11</sup> R.D. King-Smith and D. Vanderbilt, “Theory of polarization of crystalline solids,” *Phys. Rev. B* **47**, 1651–1654 (1993).
- <sup>12</sup> C. L. Kane and E. J. Mele, “ $\mathbb{Z}_2$  topological order and the quantum spin hall effect,” *Phys. Rev. Lett.* **95**, 146802 (2005).
- <sup>13</sup> Liang Fu, C. L. Kane, and E. J. Mele, “Topological insulators in three dimensions,” *Phys. Rev. Lett.* **98**, 106803 (2007).
- <sup>14</sup> D. Xiao, M.C. Chang, and Q. Niu, “Berry phase effects on electronic properties,” *Rev. Mod. Phys.* **82**, 1959–2007 (2010).
- <sup>15</sup> Rui Yu, Wei Zhang, Hai-Jun Zhang, Shou-Cheng Zhang, Xi Dai, and Zhong Fang, “Quantized anomalous hall effect in magnetic topological insulators,” *Science* **329**, 61–64 (2010).
- <sup>16</sup> Cui-Zu Chang, Jinsong Zhang, Xiao Feng, Jie Shen, Zuo-cheng Zhang, Minghua Guo, Kang Li, Yunbo Ou, Pang Wei, Li-Li Wang, Zhong-Qing Ji, Yang Feng, Shuaihua Ji, Xi Chen, Jinfeng Jia, Xi Dai, Zhong Fang, Shou-Cheng

- Zhang, Ke He, Yayu Wang, Li Lu, Xu-Cun Ma, and Qi-Kun Xue, “Experimental observation of the quantum anomalous hall effect in a magnetic topological insulator,” *Science* **340**, 167–170 (2013).
- <sup>17</sup> F. D. M. Haldane, “Attachment of surface ”fermi arcs” to the bulk fermi surface: ”fermi-level plumbing” in topological metals,” [arXiv:1401.0529](https://arxiv.org/abs/1401.0529) (2014).
- <sup>18</sup> ZK Liu, LX Yang, SC Wu, C Shekhar, J Jiang, HF Yang, Y Zhang, SK Mo, Z Hussain, B Yan, C Felser, and YL Chen, “Observation of unusual topological surface states in half-heusler compounds LnPtBi (Ln=Lu,Y),” *Nat. Commun.* **7**, 12924 (2016).
- <sup>19</sup> Shuichi Murakami, “Phase transition between the quantum spin hall and insulator phases in 3d: emergence of a topological gapless phase,” *New J. Phys.* **9**, 356 (2007).
- <sup>20</sup> Xiangang Wan, Ari M. Turner, Ashvin Vishwanath, and Sergey Y. Savrasov, “Topological semimetal and fermi-arc surface states in the electronic structure of pyrochlore iridates,” *Phys. Rev. B* **83**, 205101 (2011).
- <sup>21</sup> Gang Xu, Hongming Weng, Zhijun Wang, Xi Dai, and Zhong Fang, “Chern semimetal and the quantized anomalous hall effect in HgCr<sub>2</sub>Se<sub>4</sub>,” *Phys. Rev. Lett.* **107**, 186806 (2011).
- <sup>22</sup> Kai-Yu Yang, Yuan-Ming Lu, and Ying Ran, “Quantum hall effects in a weyl semimetal: Possible application in pyrochlore iridates,” *Phys. Rev. B* **84**, 075129 (2011).
- <sup>23</sup> A. A. Burkov and Leon Balents, “Weyl semimetal in a topological insulator multilayer,” *Phys. Rev. Lett.* **107**, 127205 (2011).
- <sup>24</sup> William Witczak-Krempa and Yong Baek Kim, “Topological and magnetic phases of interacting electrons in the pyrochlore iridates,” *Phys. Rev. B* **85**, 045124 (2012).
- <sup>25</sup> Su-Yang Xu, Nasser Alidoust, Ilya Belopolski, Zhujun Yuan, Guang Bian, Tay-Rong Chang, Hao Zheng, Vladimir N Strocov, Daniel S Sanchez, Guoqing Chang, Chenglong Zhang, Daixiang Mou, Yun Wu, Lunan Huang, Chi-Cheng Lee, Shin-Ming Huang, BaoKai Wang, Arun Bansil, Horng-Tay Jeng, Titus Neupert, Adam Kaminski, Hsin Lin, Shuang Jia, and Zahid M. Hasan, “Discovery of a weyl fermion state with fermi arcs in niobium arsenide,” *Nature Phys.* **11**, 748 (2015).
- <sup>26</sup> B. Q. Lv, H. M. Weng, B. B. Fu, X. P. Wang, H. Miao, J. Ma, P. Richard, X. C. Huang, L. X. Zhao, G. F. Chen, Z. Fang, X. Dai, T. Qian, and H. Ding, “Experimental discovery of weyl semimetal taas,” *Phys. Rev. X* **5**, 031013 (2015).
- <sup>27</sup> Ling Lu, Zhiyu Wang, Dexin Ye, Lixin Ran, Liang Fu, John D. Joannopoulos, and Marin Soljačić, “Experimental observation of Weyl points,” *Science* **349**, 622–624 (2015).
- <sup>28</sup> Barry Bradlyn, L Elcoro, Jennifer Cano, MG Vergniory, Zhijun Wang, C Felser, MI Aroyo, and B Andrei Bernevig, “Topological quantum chemistry,” *Nature* **547**, 298 (2017).
- <sup>29</sup> N. P. Armitage, E. J. Mele, and Ashvin Vishwanath, “Weyl and dirac semimetals in three-dimensional solids,” *Rev. Mod. Phys.* **90**, 015001 (2018).
- <sup>30</sup> Yi Li and F. D. M. Haldane, “Topological nodal cooper pairing in doped weyl metals,” *Phys. Rev. Lett.* **120**, 067003 (2018).
- <sup>31</sup> Shuichi Murakami and Naoto Nagaosa, “Berry phase in magnetic superconductors,” *Phys. Rev. Lett.* **90**, 057002 (2003).
- <sup>32</sup> Paul Adrien Maurice Dirac, “Quantised singularities in the electromagnetic field,” *Proc. R. Soc. Lond. A.* **133**, 60–72 (1931).
- <sup>33</sup> Ig Tamm, “Die verallgemeinerten Kugelfunktionen und die Wellenfunktionen eines Elektrons im Felde eines Magnetpoles,” *Zeitschrift Für Physik* **71**, 141–150 (1931).
- <sup>34</sup> Tai Tsun Wu and Chen Ning Yang, “Dirac monopole without strings: Monopole harmonics,” *Nucl. Phys. B* **107**, 365 – 380 (1976).
- <sup>35</sup> F. D. M. Haldane, “Fractional quantization of the hall effect: A hierarchy of incompressible quantum fluid states,” *Phys. Rev. Lett.* **51**, 605–608 (1983).
- <sup>36</sup> Eric Bobrow, Canon Sun, and Yi Li, “Monopole charge density wave states in weyl semimetals,” *Phys. Rev. Res.* **2**, 012078 (2020).
- <sup>37</sup> N. Read and D. Green, “Paired states of fermions in two dimensions with breaking of parity and time-reversal symmetries and the fractional quantum Hall effect,” *Phys. Rev. B* **61**, 10267–10297 (2000).
- <sup>38</sup> L. Fu and CL Kane, “Superconducting proximity effect and Majorana fermions at the surface of a topological insulator,” *Phys. Rev. Lett.* **100**, 96407 (2008).
- <sup>39</sup> A.P. Schnyder, S. Ryu, A. Furusaki, and A.W.W. Ludwig, “Classification of topological insulators and superconductors in three spatial dimensions,” *Phys. Rev. B* **78**, 195125 (2008).
- <sup>40</sup> Suk Bum Chung and Shou-Cheng Zhang, “Detecting the majorana fermion surface state of he 3- b through spin relaxation,” *Phys. Rev. Lett.* **103**, 235301 (2009).
- <sup>41</sup> Roman M Lutchyn, Jay D Sau, and S Das Sarma, “Majorana fermions and a topological phase transition in semiconductor-superconductor heterostructures,” *Phys. Rev. Lett.* **105**, 077001 (2010).
- <sup>42</sup> Xiao-Liang Qi and Shou-Cheng Zhang, “Topological insulators and superconductors,” *Rev. Mod. Phys.* **83**, 1057–1110 (2011).
- <sup>43</sup> Jason Alicea, “New directions in the pursuit of majorana fermions in solid state systems,” *Reports on Progress in Physics* **75**, 076501 (2012).
- <sup>44</sup> Masatoshi Sato and Yoichi Ando, “Topological superconductors: a review,” *Reports on Progress in Physics* **80**, 076501 (2017).
- <sup>45</sup> M. Nielsen *et al.*, “Absence of neutrinos on a lattice:(I). Proof by homotopy theory,” *Nucl. Phys. B* **185**, 20–40 (1981).
- <sup>46</sup> M. Nielsen *et al.*, “Absence of neutrinos on a lattice:(II). Intuitive topological proof,” *Nucl. Phys. B* **193**, 173–194 (1981).
- <sup>47</sup> N. D. Mermin and Tin-Lun Ho, “Circulation and angular momentum in the A phase of superfluid helium-3,” *Phys. Rev. Lett.* **36**, 594–597 (1976).
- <sup>48</sup> Yi Li, Kenneth Intriligator, Yue Yu, and Congjun Wu, “Isotropic landau levels of dirac fermions in high dimensions,” *Phys. Rev. B* **85**, 085132 (2012).
- <sup>49</sup> Brandon M. Anderson, Gediminas Juzeliūnas, Victor M. Galitski, and I. B. Spielman, “Synthetic 3d spin-orbit coupling,” *Phys. Rev. Lett.* **108**, 235301 (2012).
- <sup>50</sup> Alan Robert Edmonds, *Angular momentum in quantum mechanics* (Princeton university press, 1957).
- <sup>51</sup> J. K. Jain, “Composite-fermion approach for the fractional quantum hall effect,” *Phys. Rev. Lett.* **63**, 199–202 (1989).
- <sup>52</sup> Tai Tsun Wu and Chen Ning Yang, “Some properties of monopole harmonics,” *Phys. Rev. D* **16**, 1018–1021 (1977).
- <sup>53</sup> R. Jackiw and C. Rebbi, “Solitons with fermion number 1/2,” *Phys. Rev. D* **13**, 3398–3409 (1976).

# Supplemental Material for ‘‘Berry Phase Enforced Spinor Pairing Order’’

Yi Li and Grayson R. Frazier

*Department of Physics and Astronomy, Johns Hopkins University, Baltimore, Maryland 21218, USA*

## S1. PROJECTED SPINOR MONOPOLE PAIRING ORDER

We derive the low-energy pairing order in the weak-coupling regime upon projecting to the states at the Fermi surface. Consider the mean-field pairing Hamiltonian in Eq. (5) in the main text, describing inter-Fermi surface pairing. As the system preserves spin-orbit coupled rotational symmetry, the inter-Fermi surface spinor pairing gap function can be expanded into partial wave channels,  $\Delta(\mathbf{k}) = \sum_{j,j_z} \Delta_{j,j_z}(\mathbf{k})$ . Due to broken inversion symmetry, each total angular momentum  $j$ ,  $j_z$  channel decomposes into two channels of opposite parity,  $l = j - 1/2$  and  $l + 1 = j + 1/2$ , as  $\Delta_{j,j_z}(\mathbf{k}) = \Delta_{j,j_z;l}(\mathbf{k}) + \Delta_{j,j_z;l+1}(\mathbf{k})$ , in which

$$\begin{aligned} \Delta_{j,j_z;l,\alpha}(\mathbf{k}) &= \Delta_{j,j_z;l}(k) \left\langle j, j_z \left| l, m = j_z - \alpha; \frac{1}{2}, \alpha \right\rangle Y_{lm}(\hat{\mathbf{k}}) \otimes |\alpha\rangle, \\ &= \Delta_{j,j_z;l}(k) \phi_{j,j_z;l,\alpha}(\hat{\mathbf{k}}). \end{aligned} \quad (\text{S1})$$

Here,  $\Delta_{j,j_z;l}(k)$  is the pairing amplitude,  $\langle j, j_z | l, m; \frac{1}{2}, \alpha \rangle$  is the Clebsch-Gordan coefficient, and  $\phi_{j,j_z;l,\alpha} = \langle j, j_z | l, m; 1/2, \alpha \rangle Y_{lm}(\hat{\mathbf{k}}) \otimes |\alpha\rangle$  is the spin spherical harmonic<sup>50</sup> with spin component  $\alpha = \pm 1/2$ .

Let us now consider the pairing between Fermi surfaces  $\text{FS}_{c,+}$  and  $\text{FS}_d$  of Eq. (4) of the main text, which have Chern numbers  $-1$  and  $0$  respectively. This inter-Fermi surface pairing can arise when the Fermi surface matching condition is satisfied, *i.e.*  $k_{F;c,+} \approx k_{F;d}$ . We define the projected pairing order as

$$P^{(+)} \Delta(\mathbf{k}) \equiv \Delta^{(+)}(\mathbf{k}) = \langle \lambda_+ | \Delta(\mathbf{k}) | d \rangle, \quad (\text{S2})$$

with  $|\lambda_+\rangle$  being the helical eigenstate  $\text{FS}_{c,+}$  and  $|d\rangle$  the eigenstate of  $\text{FS}_d$ . The band eigenstate at  $\text{FS}_{c,+}$  can be expressed in terms of half-integer monopole harmonics,

$$|\lambda_+\rangle = \begin{pmatrix} \sqrt{2\pi} Y_{\frac{1}{2}; \frac{1}{2}, -\frac{1}{2}}(\hat{\mathbf{k}}) \\ -\sqrt{2\pi} Y_{\frac{1}{2}; \frac{1}{2}, +\frac{1}{2}}(\hat{\mathbf{k}}) \end{pmatrix} = \begin{pmatrix} \cos \frac{\theta_{\mathbf{k}}}{2} e^{-i\phi_{\mathbf{k}}} \\ \sin \frac{\theta_{\mathbf{k}}}{2} \end{pmatrix}, \quad (\text{S3})$$

which have been expressed in a gauge for which the state is well-defined at the south pole. For a given partial wave channel  $l$ , the projection is given by

$$\begin{aligned} P^{(+)} \Delta_{j,j_z;l}(\mathbf{k}) &= -\Delta_{j,j_z;l}(k) \sum_{\alpha=\uparrow,\downarrow} \left\langle j, j_z \left| l, m = j_z - \alpha; \frac{1}{2}, \alpha \right\rangle \times \\ &\sum_{j'} (-1)^{j'-l+\frac{1}{2}} \sqrt{\frac{2l+1}{2j'+1}} \left\langle \frac{1}{2}, \alpha; l, m \left| j', j_z \right\rangle \left\langle \frac{1}{2}, -\frac{1}{2}; l, 0 \left| j', -\frac{1}{2} \right\rangle Y_{-\frac{1}{2}; j', j_z}(\hat{\mathbf{k}}), \end{aligned} \quad (\text{S4})$$

in which the sum is over  $j' = |l - 1/2|, l + 1/2$ . Here, we have employed the formula of product of two monopole harmonics<sup>52</sup>. The projected pairing gap function is given by

$$P^{(+)} \Delta_{j,j_z;l=j\pm\frac{1}{2}}(\mathbf{k}) = \mp \frac{1}{\sqrt{2}} \Delta_{j,j_z;l}(k) Y_{-\frac{1}{2}; j, j_z}(\hat{\mathbf{k}}), \quad (\text{S5})$$

in which we have used  $\langle l, j_z - \frac{1}{2}; \frac{1}{2}, \frac{1}{2} | l \pm \frac{1}{2}, j_z \rangle = \pm \sqrt{1/2 \mp j_z / (2l + 1)}$  and  $\langle l, (j_z + \frac{1}{2}); \frac{1}{2}, -\frac{1}{2} | l \pm \frac{1}{2}, j_z \rangle = \sqrt{1/2 \mp j_z / (2l + 1)}$ . In other words, when the pairing has the symmetry of the spinor spherical harmonic  $\phi_{j,j_z;l}(\hat{\mathbf{k}})$ , the projected pairing order belongs to the same conserved partial wave channel  $j$  with  $z$ -component angular momentum  $j_z$ . The overall sign is dependent on the partial wave channel  $l = j \pm 1/2$ . Moreover, the projected pairing order always belongs to the topological sector defined by the pair monopole charge,  $q_{\text{pair}} = -1/2$ . Analogous results hold when instead  $\text{FS}_{c,-}$  and  $\text{FS}_d$  are paired, but with the projected pairing order instead in the topological sector set by  $q_{\text{pair}} = 1/2$ .

## S2. TIGHT-BINDING MODEL OF SPINOR SUPERCONDUCTOR

We consider a three-band tight-binding BdG model describing a monopole spinor superconductor in a cubic lattice as follows:

$$H = \sum_{\mathbf{n}, \sigma, \mathbf{n}', \sigma'} c_{\mathbf{n}, \sigma}^\dagger [\mathcal{H}_c^0]_{\mathbf{n}, \sigma; \mathbf{n}', \sigma'} c_{\mathbf{n}', \sigma'} + \sum_{\mathbf{n}, \mathbf{n}'} d_{\mathbf{n}}^\dagger [\mathcal{H}_d^0]_{\mathbf{n}; \mathbf{n}'} d_{\mathbf{n}'} + \sum_{\mathbf{n}, \sigma} (\Delta_\sigma c_{\mathbf{n}, \sigma}^\dagger d_{\mathbf{n}}^\dagger + \text{h.c.}). \quad (\text{S6})$$

Here,  $\mathcal{H}_c^0$  and  $\mathcal{H}_d^0$  are the tight-binding band Hamiltonian kernels corresponding to the continuum ones for spinful  $c$  fermion and spinless  $d$  fermion, respectively.  $c_{\mathbf{n}, \sigma}$  ( $d_{\mathbf{n}}$ ) is the annihilation operator of  $c$  fermion with spin  $\sigma$  (spinless  $d$  fermion) at site  $\mathbf{n}$ . For matrix elements of  $\mathcal{H}_c^0$ , we take the following tensor product basis representation, with the two-dimensional spin- $\uparrow, \downarrow$  basis labelled by  $\sigma$  nested under lattice site basis indexed by  $\mathbf{n}$ . The nonvanishing elements of  $\mathcal{H}_c^0$  are given by

$$[\mathcal{H}_c^0]_{\mathbf{n}, \mathbf{n}} = -\mu_c \sigma_0, \quad [\mathcal{H}_c^0]_{\mathbf{n}, \mathbf{n} + \delta_i} = t_c \sigma_0 - \frac{i}{2} \lambda \sigma_i, \quad (\text{S7})$$

and the nonvanishing elements of  $\mathcal{H}_d^0$  are given by

$$[\mathcal{H}_d^0]_{\mathbf{n}, \mathbf{n}} = -\mu_d, \quad [\mathcal{H}_d^0]_{\mathbf{n}, \mathbf{n} + \delta_i} = t_d. \quad (\text{S8})$$

Above,  $\delta_i$  with  $i = x, y, z$ , are the lattice vectors denoting nearest-neighbour hopping, and spin-independent hopping amplitudes are given by  $t_c$  and  $t_d$ . We take  $t_c/2 = t_d = t = -1$ .

As we are considering only inter-Fermi surface pairing, we employ the following reduced Bogoliubov-de Gennes (BdG) Hamiltonian in the  $(\mathbf{c}_\uparrow, \mathbf{c}_\downarrow, \mathbf{d}^\dagger)^T$  Nambu basis,

$$\mathcal{H}_{\text{BdG}} = \left( \begin{array}{cc|c} \mathcal{H}_c^0 & & \begin{array}{c} \Delta_\uparrow \\ \Delta_\downarrow \end{array} \\ \hline \Delta_\uparrow^\dagger & \Delta_\downarrow^\dagger & -\mathcal{H}_d^0 \end{array} \right), \quad (\text{S9})$$

with  $\mathbf{c}_\uparrow$ ,  $\mathbf{c}_\downarrow$ , and  $\mathbf{d}^\dagger$  being a shortened notation including site indices. The Fourier transform of the above tight-binding models is given by

$$\mathcal{H}_d^0(\mathbf{k}) = -\mu_d + \sum_i 2t_d \cos k_i, \quad (\text{S10})$$

$$\mathcal{H}_c^0(\mathbf{k}) = -\mu_c \sigma_0 + \sum_i (2t_c \cos k_i \sigma_0 - \lambda \sin k_i \sigma_i). \quad (\text{S11})$$

In the continuum limit, the above band Hamiltonians simplify to those in Eq. (4) of the main text. In the following tight-binding model, we consider the case when the superconducting pairing is on-site, where  $\Delta_\alpha = \mathbb{1} \Delta_\alpha$  with  $\alpha = \uparrow, \downarrow$ . Such pairing can occur for a simple contact interaction, as described in Eq. (7) of the main text.

### A. Pairing between $\text{FS}_{c,+}$ and $\text{FS}_d$

We first consider the case in which Fermi surfaces  $\text{FS}_{c,+}$  and  $\text{FS}_d$  are paired. To satisfy the Fermi surface matching condition, we take  $\mu_d = 2t_d(\cos k_F + 2)$  and  $\mu_c = 2t_c(\cos k_F + 2) + \lambda|\sin k_F|$ , with  $k_F = k_{F;c,+} = k_{F;d}$  being the Fermi wavevector of  $\text{FS}_{c,+}$  and  $\text{FS}_d$ , and  $t = t_c = t_d/2$  being the spin-independent hopping amplitude. Although there are small deviations from a spherical Fermi surface due to the lattice symmetry, the pairing between  $\text{FS}_{c,+}$  and  $\text{FS}_d$  is energetically preferable over that between  $\text{FS}_{c,-}$  and  $\text{FS}_d$ . We consider inter-Fermi surface pairing  $\mathbf{\Delta}(\mathbf{k}) = (\Delta_0, 0)$ , with  $\Delta_0$  being the pairing amplitude.

In Fig. 2 (a) of the main text, we show the bulk BdG dispersion for the tight-binding model. Near the north pole at  $(0, 0, k_F)$ , the system is gapped. In contrast, at the south pole at  $(0, 0, -k_F)$ , there is a single emergent BdG node, and the BdG state has local chiral  $p$ -wave symmetry in momentum space near the gap node. The single emergent BdG node leads to nonvanishing odd vorticity,  $\nu = -1$ , corresponding to twice the half-integer pair monopole charge,  $q_{\text{pair}} = -1/2$ . The single emergent Weyl node arises from the pairing of  $\text{FS}_{c,+}$  and  $\text{FS}_d$  in the weak-coupling regime. The pairing between states of  $\text{FS}_{c,-}$  and  $\text{FS}_d$  is energetically unfavorable in the weak-coupling regime due to the Fermi surface mismatch. Hence, states of  $\text{FS}_{c,-}$  remain unpaired and do not contribute to the low-energy pairing order.



We study the zero energy surface modes using the tight-binding model. Under periodic boundary conditions along  $y$  and  $z$  directions, at given conserved momenta  $k_y$  and  $k_z$ , the system is effectively a 1D system with open boundaries along  $x$  direction. In Fig. 2 (b) of the main text, we show the zero energy surface arc states appearing close to the southern hemisphere of projected Fermi surface in the surface Brillouin zone. Such surface states arise from the local  $p_x + ip_y$  symmetry of the monopole pairing order near the gap node. Analogous to the Jackiw-Rebbi model<sup>53</sup>, the nontrivial winding of local pairing phase leads to zero energy states located at surface. Moreover, the zero energy surface arc originates from the single pairing gap node at the south pole before merging into the unpaired  $\text{FS}_{c,-}$  bulk states, which is a unique characterization of this spinor pairing order.

Furthermore, we present the dispersion of the surface states obtained with the tight-binding model in Fig. 3 of the main text. In Fig. 3 (a), the surface states are computed for conserved momentum  $k_z = -0.22\pi$  satisfying  $k_{F;c,-} < k_z < k_{F;c,+} = k_{F;d}$ . There are two distinct surface states localized to opposite sides of the sample. The surface state at  $x = 0$  ( $x = L_x$ ) has negative (positive) group velocity and manifests the local  $p_x + ip_y$  symmetry of the pairing order near the pairing gap node. In Fig. 3 (b), for  $k_z = 0.16\pi < k_{F;c,-}$ , the bulk states of the unpaired  $\text{FS}_{c,-}$  are also present at zero energy. Nonetheless, the surface states prevail, and as manifested by the group velocity of the surface state, the local  $p_x + ip_y$  symmetry is unchanged. For  $k_z$  sufficiently less than  $k_{F;c,-}$ , for example  $k_z = -0.10\pi$  shown in Fig. 3 (c), the surface states are no longer at zero energy and have merged into the bulk unpaired Fermi surface,  $\text{FS}_{c,-}$ .

### B. Pairing between $\text{FS}_{c,-}$ and $\text{FS}_d$

To complement the above discussion, we now consider when pairing is instead between  $\text{FS}_{c,-}$  and  $\text{FS}_d$ . This can be achieved by adjusting the chemical potential so that  $\mu_d = 2t_d(\cos k_{F;c,-} + 2)$  and  $\mu_c = 2t_c(\cos k_{F;c,-} + 2) - \lambda|\sin k_{F;c,-}|$ , with  $k_{F;c,-}$  being the Fermi wavevector of  $\text{FS}_{c,-}$ . Because  $\text{FS}_{c,-}$  has the opposite Chern number of  $\text{FS}_{c,+}$ , the pair monopole charge of the Cooper pair is now given by  $q_{\text{pair}} = 1/2$ . In analogy to Eq. (9) of the main text, let us consider the BdG excitations when the inter-Fermi surface pairing is given by  $\mathbf{\Delta} = (\Delta_0, 0)^T$ , with  $\Delta_0$  being the pairing amplitude. In the continuum limit, the low-energy BdG Hamiltonian in the Nambu basis of  $\psi(\mathbf{k}) = (\chi_-(\mathbf{k}), d^\dagger(-\mathbf{k}))^T$  is given by

$$\mathcal{H}(\mathbf{k}) = \epsilon_{0,k}\tau_0 + \epsilon_k\tau_3 + \sqrt{2\pi}\Delta_0 Y_{\frac{1}{2},\frac{1}{2},\frac{1}{2}}(\hat{\mathbf{k}})\tau_+ + \sqrt{2\pi}\Delta_0 Y_{\frac{1}{2},\frac{1}{2},\frac{1}{2}}^*(\hat{\mathbf{k}})\tau_- . \quad (\text{S12})$$

Above,  $\epsilon_{0,k} = (\epsilon_{k;c,-} - \epsilon_{k;d})/2$  and  $\epsilon_k = (\epsilon_{k;c,-} + \epsilon_{k;d})/2$ , with  $\epsilon_{k;c,-} = \hbar^2 k^2/(2m) + \lambda k - \mu_c$  and  $\epsilon_{k;d} = \hbar^2 k^2/(2M) - \mu_d$  being the dispersions of the band eigenstates at the Fermi level. Here, the low-energy pairing order has the symmetry of the monopole harmonic  $Y_{\frac{1}{2},\frac{1}{2},\frac{1}{2}}(\hat{\mathbf{k}}) = \sin(\theta_{\mathbf{k}}/2)e^{i\phi_{\mathbf{k}}}$ , which has a single point node at the north pole. Near the gap node, the pairing order has local  $p_x + ip_y$  symmetry, and the total vorticity is given by  $\nu = 2q_{\text{pair}} = 1$ .

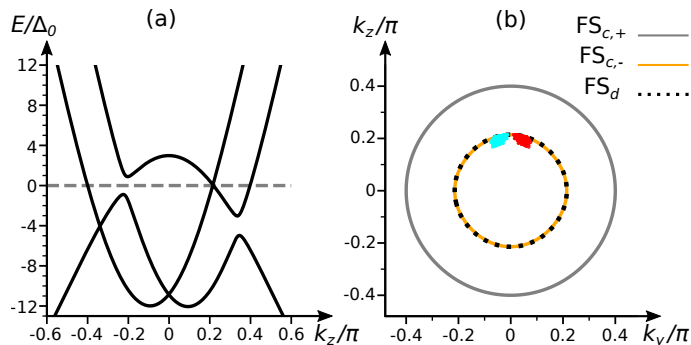


FIG. S1. (a) Bulk BdG spectrum of the three-band tight-binding model of spinor superconductor along  $k_z$  axis. The BdG spectra exhibits a single BdG Weyl node at  $k_z = k_{F;c,-} = k_{F;d} = 0.67$ . (b) zero energy surface arcs (colored) within 2D surface Brillouin zone. States localized at  $x = 0$  ( $x = L_x$ ) are shown in red (cyan). Overlaid are the  $k_x = 0$  cross sections of bulk Fermi surfaces,  $\text{FS}_d$  (dashed black line),  $\text{FS}_{c,+}$  (solid gray line), and  $\text{FS}_{c,-}$  (solid orange line). Parameters are the same as that of Fig. 2 of the main text, but now with  $\mu_c/t = 10.38$  and  $\mu_d/t = 5.56$ , with  $k_{F;c,-} = 0.67$  being the wave vector of the paired  $\text{FS}_{c,-}$ .

In Fig. S1 (a), we show the dispersion of the BdG quasiparticle states for the tight-binding model. Near the south pole, the pairing is fully gapped, whereas as at the north pole, there is now a single BdG Weyl node. Due to the Fermi surface matching condition, pairing between  $\text{FS}_{c,+}$  and  $\text{FS}_d$  is now energetically unfavorable. The results are

analogous to that of Fig. 2 of the main text; only here, due to the Fermi surface matching condition between  $\text{FS}_{c,-}$  and  $\text{FS}_d$ , the BdG node is now at the north pole, at  $k_{F;c,-\hat{z}}$ .

We study the low-energy excitations of the tight-binding BdG Hamiltonian and demonstrate the single emergent BdG Weyl node. Expanded near the BdG node at  $(0, 0, k_{F;c,-})$ , the BdG Hamiltonian in the Nambu basis of  $\psi(\mathbf{k}) = (\chi_-(\mathbf{k}), d^\dagger(-\mathbf{k}))$  is given by

$$\mathcal{H}(\mathbf{k}) \equiv \mathcal{H}(k_{F;c,-\hat{z}} + \tilde{\mathbf{k}}) \approx \begin{pmatrix} -(2t_c \sin k_{F;c,-} - \lambda \cos k_{F;c,-})\tilde{k}_z & \frac{\Delta_0}{2|\sin k_{F;c,-}|}(\tilde{k}_x + i\tilde{k}_y) \\ \frac{\Delta_0}{2|\sin k_{F;c,-}|}(\tilde{k}_x - i\tilde{k}_y) & 2t_d \sin(k_{F;c,-})\tilde{k}_z \end{pmatrix}. \quad (\text{S13})$$

Here, the pairing order has local  $p_x + ip_y$  symmetry near the gap node. In Fig. S1 (b), we show the zero energy surface states in the surface Brillouin zone. Near the projected gap node at  $k_{F;c,-\hat{z}}$ , the nontrivial pairing phase winding in momentum space gives rise to surface modes localized at opposite surfaces. These states originate from the BdG Weyl node but quickly merge into the bulk zero energy states of the unpaired  $\text{FS}_{c,+}$ . The origin of the nontrivial surface states are the same as that discussed in Sec. S2 A, with the difference being the location of the emergent BdG Weyl node and the net vorticity.